

## Effect of NaNO<sub>2</sub>, HNO<sub>3</sub> and H<sub>2</sub>SO<sub>4</sub> on the structure and reactivity of $\gamma$ -alumina

Abdol Hossein Dabbagh<sup>a</sup>, Marzie Naderi<sup>a</sup>, Mehdi Zamani<sup>b,\*</sup>

<sup>a</sup>Department of Chemistry, Isfahan University of Technology, Isfahan 84156-83111, Iran.

<sup>b</sup>School of Chemistry, Damghan University, 36716-41167 Damghan, Iran.

Received 5 March 2019; received in revised form 27 September 2019; accepted 6 October 2019

### ABSTRACT

The influence of NaNO<sub>2</sub>, HNO<sub>3</sub> and H<sub>2</sub>SO<sub>4</sub> on the structure and morphology of  $\gamma$ -alumina was investigated by XRD, BET, SEM and FT-IR spectroscopy. Selected amounts of NaNO<sub>2</sub>, HNO<sub>3</sub> and H<sub>2</sub>SO<sub>4</sub> were added to a solution of aluminum isopropoxide (as a precursor for the boehmite synthesis). The boehmite samples were calcined at 350 and 600 °C to form the semi-crystalline high surface area  $\gamma$ -Al<sub>2</sub>O<sub>3</sub>. The reactivity and selectivity of the modified  $\gamma$ -alumina catalysts were examined using dehydration reaction of 2-octanol. There was a good correlation between reactivity, selectivity and the amounts (and type) of the modification. The dominant product was *cis*-2-octene for all of the catalysts. Low conversion and high selectivity were obtained for dehydration of 2-octanol over alumina modified with NaNO<sub>2</sub>. High conversion, low selectivity and excessive isomerization were found for  $\gamma$ -alumina catalyst modified with H<sub>2</sub>SO<sub>4</sub>.

**Keywords:** Alumina, Dehydration, Alcohol, Reactivity, Selectivity.

### 1. Introduction

$\gamma$ -Alumina is excellent and widely used catalyst for dehydration of alcohols [1-10]. Many discrepancies have resulted from different catalytic properties of the aluminum precursor used in different laboratories and/or from different reaction conditions. These catalysts can vary widely in their activity for skeletal isomerization and for double-bond shift of olefinic hydrocarbons.

The mode of elimination for the dehydration reaction over  $\gamma$ -alumina catalyst has been shown to be *anti* from the antiperiplanar conformation with preference to form the *cis* isomer, when there is the possibility to form geometric isomers [7]. A new transition-state model has been developed by Dabbagh and Mohammad Salehi in order to justify the *anti*-intramolecular *E2* elimination with *cis* (*Z*)-preference over pure alumina and intermolecular *E2* elimination with *trans* (*E*)-preference over modified alumina. The reactions of model compounds over aluminum oxides were reported at 200-350 °C and in the pH range of 4.5-9.5 [7].

It was concluded that the stereochemistry of elimination reaction depends on not only to the steric interaction of the intermediate and/or transition state, but on pH and the temperature. Recently, density functional theory (DFT) study for dehydration mechanism of 2-butanol over (1 0 0) surface and nanochannel of  $\gamma$ -alumina clarified several hidden aspects of  $\gamma$ -alumina surface [11]. It was found that the *E2* elimination with a synclinal transition state is comparable with an *E2* antiperiplanar transition state. Roy et al. reported the mechanistic study of alcohols dehydration over  $\gamma$ -alumina [12]. They demonstrated that the  $\gamma$ -alumina acts as a Lewis acid in its interactions with simple alcohols and water simply blocks the reactive sites but does not introduce Brønsted acidity. Reaction of adsorbed alcohols occurs through a transition state that has carbenium-ion character, as demonstrated by both DFT calculations and measured activation energies for reaction of various adsorbed alcohols. Finally, alkali impurities significantly affected the reactivity of  $\gamma$ -alumina [12].

Understanding the complex nature of  $\gamma$ -alumina structure and the way atoms arrange in space has been the cornerstone of investigations for the past century. The nature of active sites has gained most of the

\*Corresponding author.

Email: m.zamani@du.ac.ir (M. Zamani)

attention due to their important roles in chemical reactions. Several interpretations of the nature of active sites on the surface of  $\gamma$ -alumina are available [13]. The widely accepted model, proposed by Peri, assumes a random configuration of hydroxyl groups after dehydration leaving adjoining residual oxide ions, oxide vacancies and exposed aluminum ions [14]. Also, some structural models of  $\gamma$ -alumina such as defect spinel, hydrogenated spinel and non-spinel models have been reported based on the single crystal X-ray and theoretical calculations [15-24].

$\gamma$ -Alumina is generally produced by calcination of aluminum oxy-hydroxide (boehmite) at 500-700 °C [25]. Recently, the preparation of  $\gamma$ -alumina at lower temperatures (i.e. 350 °C) have been reported by Dabbagh et al. [10]. Amini and Mirzaee have reported the preparation of boehmite and  $\gamma$ -alumina using various aluminum alkoxide precursors [26]. Le Bihan et al. have examined the influence of the chelating agents such as butan-1,3-diol and acetylacetone in aluminum isopropoxide solution [27]. A decrease in the crystallinity of alumina was observed with increasing amount of complexing agent [27]. Takeda et al. have studied the effect of HNO<sub>3</sub> and HCl on crystalline structure of alumina prepared by the hydrolysis of tri-N-butylaluminum oxide at 600-900 °C [28]. They reported that NO<sub>3</sub><sup>-</sup> ions assisted the building of a gel structure in which aluminum or oxide ions was readily diffused at temperatures higher than 800 °C [28]. The effect of pH on the size of crystalline and other properties of boehmite was investigated by Okada et al. [29]. The X-ray diffraction (XRD) patterns predicted boehmite and bayerite crystals at pH = 7-10 and 11, respectively [29]. Parida et al. prepared and characterized nano size  $\gamma$ -alumina using ammonium bicarbonate, ammonium carbonate, sodium bicarbonate and sodium carbonate [30]. Addition of ammonium hydroxide was studied by Kim [31]. According to the results, the amorphous alumina was transformed to a crystalline form when calcination temperature increased to 500 °C [31]. The influence of mineral acids such as H<sub>2</sub>SO<sub>4</sub>, HCl and HNO<sub>3</sub> on the production of alumina nano powder has been investigated by Manivasakan et al. [32]. The reduced crystalline size and higher surface area was reported for the catalyst precipitated with HNO<sub>3</sub>. Most of the previous publications [26-32] were restricted to the synthesis and morphology of  $\gamma$ -alumina. A detailed understanding of the morphology and catalytic properties, which is the subject of this article, is still lacking.

Recently, the dissociative adsorption of NaNO<sub>2</sub>, NaNO<sub>3</sub>, HNO<sub>2</sub>, HNO<sub>3</sub> and H<sub>2</sub>SO<sub>4</sub> over  $\gamma$ -alumina surface was investigated by Zamani and Dabbagh using

DFT calculations [33]. They found that all of the mentioned compounds were dissociated to their ionic forms after adsorption over the surface [33]. By addition of HNO<sub>2</sub>, HNO<sub>3</sub> and H<sub>2</sub>SO<sub>4</sub>, the Lewis acidity of alumina surface was increased; while in the presence of NaNO<sub>2</sub> and NaNO<sub>3</sub>, the acidity of catalyst was decreased [33]. In this study, the influence of NaNO<sub>2</sub>, HNO<sub>3</sub> and H<sub>2</sub>SO<sub>4</sub> on the structure, morphology, reactivity and selectivity of  $\gamma$ -alumina catalyst was investigated experimentally.

## 2. Experimental

Aluminum iso-propoxide, sodium nitrate, nitric acid, sulfuric acid and 2-octanol, were purchased from Merck Chemical Co. and used as received. In all catalyst preparations, the distilled water was used as solvent.

$\gamma$ -Alumina was prepared by hydrolysis of aluminum iso-propoxide [Al(OC<sub>3</sub>H<sub>7</sub>)<sub>3</sub>] in deionized water (H<sub>2</sub>O:Al mol ratio of 100:1), in the presence HNO<sub>3</sub> (0.1, 0.5 and 1 mol), H<sub>2</sub>SO<sub>4</sub> (0.5 mol) and NaNO<sub>2</sub> (0.5 mol). The mixtures were refluxed for 6 h at room temperature. The pH of solutions was measured just after mixing. The excess water and isopropyl alcohol were removed by evaporation at 100 °C. The residues were allowed to stand at 120 °C for 48 h followed by calcinations at 350 (for 24 h) and 600 °C for 6 h. Analysis of the samples was performed at each stage.

The X-ray diffraction (XRD) patterns were acquired using a Bruker-AXS D8-Discover diffractometer with a parallel incident beam (Göbel mirror) and a vertical theta-theta goniometer, an XYZ motorized stage mounted on an Eulerian cradle, diffracted-beam Soller slits, a 0.02° receiving slit and a scintillation counter as a detector. The angular 2theta (2 $\theta$ ) diffraction range was between 5 and 80°. The data were collected with an angular step of 0.02° at 4s per step and sample rotation. CuK radiation was obtained from a copper X-ray tube operated at 40 kV and 40 mA ( $\lambda$ =1.54 Å). The pH measurements were obtained using Metrohm 827 model pH meter with calomel glass electrode. The scanning electron microscopy (SEM) images were obtained with a JEOL JSM-6400 scanning microscope operated at an acceleration voltage of 20 kV. The Fourier transform infrared (FT-IR) spectra were recorded on a Jasco-FT-IR-680 plus apparatus using KBr transparent discs. The single point Brunauer-Emmett-Teller (BET) analysis was performed using a Chembet 3000 Quantachrome apparatus at 77 K. The samples were degasified before analysis at 100 °C for 5 h. The BET method was applied to calculate total surface area.

Elimination reactions of 2-octanol were done over the prepared catalysts at 280 °C. Reactions were carried out

in a vertical plug flow reactor made of Pyrex glass and fitted with a thermal well extended to the center of the catalyst bed. About 20-30 cc of the reactor volume above the catalyst bed contained Pyrex glass beads to serve as preheater. The conversion of alcohols was maintained to the lowest level possible by using 2 g sample (0.50 g of catalyst mixed mechanically with 1.5 g of powder glass beads) [7] and pretreated in situ in air for 2 h at 400 °C, and then with dry nitrogen for 30 min. The feed consisted of 18 cm<sup>3</sup> pure alcohol per hour. Alcohol conversion and products selectivity were monitored using the Agilent 6890N gas chromatograph equipped with a capillary HP-5 column. The column properties were: 30 m long, 0.32 mm in inner diameter, and 0.25 μm film thick. The column stationary phase was (5% Phenyl)-methyl polysiloxane. The products were identified using the Fisons 8060 GC-MASS instrument equipped with a 30 m HP-5 capillary column.

### 3. Results and Discussion

The XRD patterns of the gel powders made by drying the sol-gel precursors in the presence of 0.5 mol NaNO<sub>2</sub>, HNO<sub>3</sub> and H<sub>2</sub>SO<sub>4</sub> at 120 °C are shown in Fig. 1. The typical XRD patterns show characteristic reflections of AlO(OH) at  $2\theta \cong 14$  (0 2 0), 28 (1 2 0), 38 (0 3 1), 49 (2 0 0, 0 5 1), 65 (0 0 2), 72 (2 5 1), 86° (2 0 2). All peaks correspond to the boehmite phase with an orthorhombic unit cell according to ASTM 21-1307. The XRD pattern at  $2\theta \cong 30, 32, 44$  and  $45^\circ$  show characteristic reflections of NaNO<sub>2</sub> for the sample modified by 0.5 mol NaNO<sub>2</sub> (according to ASTM 01-0883). The broad diffraction lines of all the samples indicate low crystallinity of the boehmite phase.

Fig. 2 shows the XRD patterns of samples prepared using 0.1, 0.5 and 1 mol of HNO<sub>3</sub> at 120 °C.

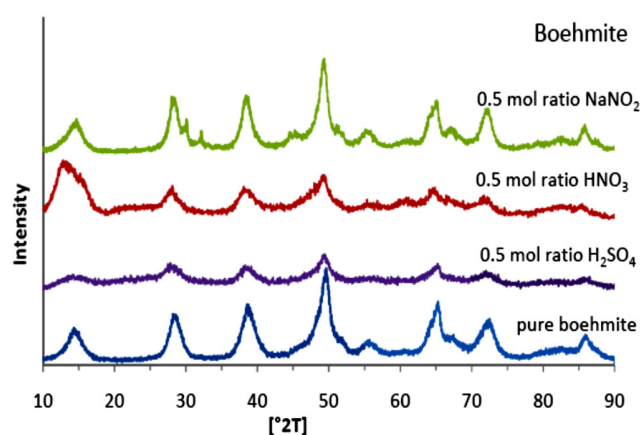


**Fig. 1.** The XRD pattern of prepared boehmite samples in the presence of 0.5 mol ratio of H<sub>2</sub>SO<sub>4</sub>, HNO<sub>3</sub> and NaNO<sub>2</sub> at 120 °C, in comparison to pure boehmite.

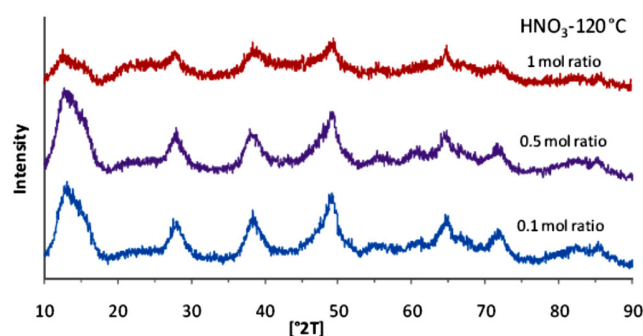


**Fig. 2.** The XRD pattern of prepared boehmite samples in the presence of 0.1, 0.5 and 1 mol ratio of HNO<sub>3</sub> at 120 °C.

The crystallinity was reduced at higher concentration of nitric acid and approached the amorphous phase in a sample using 1 mol additive. Similar XRD pattern was observed for 0.5 mol ratio of H<sub>2</sub>SO<sub>4</sub> (Fig. 1). The distance between the crystal plane ( $2\theta = 14^\circ$  (0 2 0)) of the sample modified by 1 mol of HNO<sub>3</sub> was calculated 0.71 nm.

The XRD patterns of the calcined samples at 350 °C indicate transformation of the boehmite phase to  $\gamma$ -alumina after calcination (Fig. 3). The pattern at  $2\theta = 38$  (3 1 1), 39 (2 2 2), 46 (4 0 0), and 66° (4 4 0) of the sample modified with HNO<sub>3</sub> (0.5 mol at 350 °C) corresponds to  $\gamma$ -alumina according to ASTM 10-0425. The pattern of the sample modified with H<sub>2</sub>SO<sub>4</sub> shows incomplete formation of  $\gamma$ -alumina phase at 350 °C but pattern at  $2\theta = 29$  and  $76^\circ$  predicts formation of 3Al<sub>2</sub>O<sub>3</sub>.4SO<sub>4</sub>.xH<sub>2</sub>O phase according to ASTM16-0398. The pattern at  $2\theta = 29$  and  $48^\circ$  for the sample modified with NaNO<sub>2</sub> at this temperature predicted  $\gamma$ -alumina and new NaNO<sub>3</sub> phases (according to ASTM01-0840). The XRD patterns (Fig. 4) of  $2\theta = 46$  (4 0 0) and  $66^\circ$  (4 4 0) and ( $2\theta = 38, 39, 62,$  and  $85^\circ$ ) for the catalyst modified with 0.5 mol of H<sub>2</sub>SO<sub>4</sub>, HNO<sub>3</sub> and NaNO<sub>2</sub> at 600 °C show complete transformation of boehmite to  $\gamma$ -alumina. The peak broadening is related to the amorphous morphology [34].

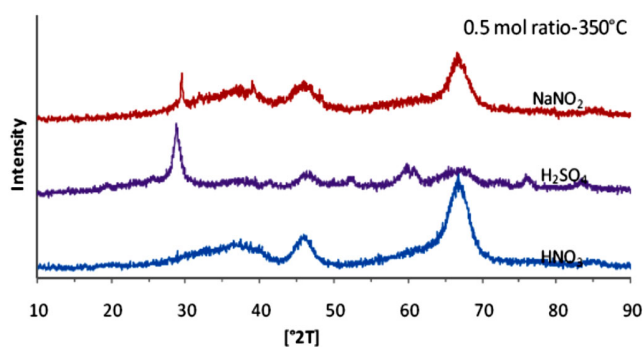


**Fig. 3.** The XRD pattern of prepared  $\gamma$ -alumina samples in the presence of 0.5 mol ratio of H<sub>2</sub>SO<sub>4</sub>, HNO<sub>3</sub> and NaNO<sub>2</sub> at 350 °C.

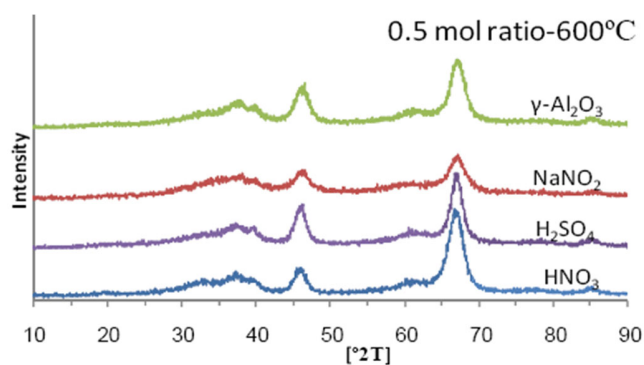


**Fig. 4.** The XRD pattern of prepared  $\gamma$ -alumina samples in the presence of 0.5 mol ratio of  $\text{NaNO}_2$ ,  $\text{H}_2\text{SO}_4$  and  $\text{HNO}_3$  at 600 °C, in comparison to pure  $\gamma$ -alumina.

The XRD patterns of  $\gamma$ -alumina prepared using 0.5 mol ratio of  $\text{HNO}_3$  at 120, 350 and 600 °C indicate substantial transformation of  $\text{AlO}(\text{OH})$  at 120 °C (loss of peaks at  $2\theta \cong 14, 19, 28, 50, 65, 72^\circ$ ) to lower crystalline phase  $\gamma$ -alumina at 350 and higher crystalline phase at 600 °C, (Fig. 5) with the broad reflections. The broadness is attributed to preparation conditions and to a random distribution of the aluminum ions over the tetrahedron sites of the spinel lattice.

The effect of heat treatment on the pH of the sol before and after reflux was measured using  $\text{HNO}_3$ ,  $\text{H}_2\text{SO}_4$ , and  $\text{NaNO}_2$  (Table 1). The pH of the sol using 0.1 mol of  $\text{HNO}_3$  and 0.5 mol of  $\text{NaNO}_2$  did not change before and after reflux. The pH was increased drastically for the sol using 0.5 mol of  $\text{HNO}_3$  and for  $\text{H}_2\text{SO}_4$  after the reflux.

The largest pH variation was observed for the sol using 1 mol  $\text{HNO}_3$  (protonation of  $\text{AlOOH}$  to  $\text{AlOOH}_2^+$ ). The microstructure of the gel is affected according to the amount of acid added during the hydrolysis which is related to the electrostatic repulsion between the boehmite particles. The surface of boehmite is fully covered by hydroxyl groups and has an amphoteric character (positively or negatively charged,  $\text{AlOH}_2^+$  or  $\text{AlO}^-$ ). The pH at which the overall charge of the water-oxide interface is close to zero is known as the point of zero charge (PZC). For boehmite powder, the PZC reported in the literature is close to 9 [34-36]. The surface charge will increase when acid is added. Increasing the electrostatic repulsion between the particles organize smaller particles.

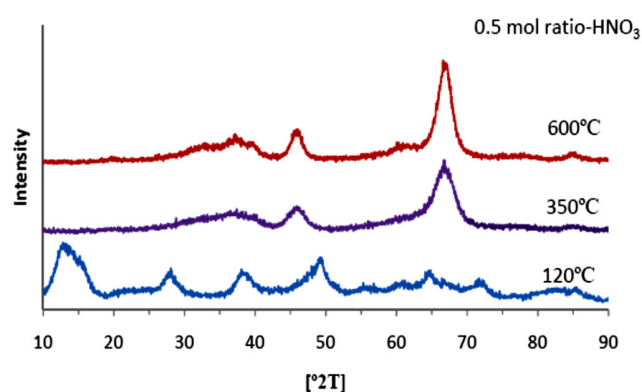


**Fig. 5.** The XRD pattern of  $\gamma$ -alumina samples prepared using 0.5 mol ratio of  $\text{HNO}_3$  at 120, 350 and 600 °C.

In the case of  $\text{H}_2\text{SO}_4$ , ( $\text{pH} = 1.25\text{-}3.34$ ) the surface charge is at maximum, causing reduced particle size which is shown by peak broadening in XRD pattern (Fig. 1). In the prepared sol using  $\text{NaNO}_2$ ,  $\text{pH} = 8.4\text{-}8.6$  which is near the PZC with low charge. The particles stick together to build larger particle size with crystalline structure.

The sol prepared with 0.5 mol of  $\text{HNO}_3$  ( $\text{pH} < \text{pH}_{\text{pzc}}$ ) at 120 °C is transparent, glass like which easily form powder. The sol prepared with 0.5 mol of  $\text{H}_2\text{SO}_4$  ( $\text{pH} < \text{pH}_{\text{pzc}}$ ) produces light powder porous material at this temperature. The sol prepared with 0.5 mol of  $\text{NaNO}_2$  ( $\text{pH} \cong \text{pH}_{\text{pzc}}$ ) produces rigid dense material which is difficult to transform to powder. These sols were treated at 350 and 600 °C for 6 h to give  $\gamma$ -alumina. The SEM images of the former two catalysts show uniform appearance. The SEM of the latter catalyst shows no uniform appearance (Fig. 6).

The BET specific surface area for the prepared  $\gamma$ -alumina samples (calcined at 600 °C) in the presence of 0.5 mol  $\text{NaNO}_2$ ,  $\text{HNO}_3$  and  $\text{H}_2\text{SO}_4$  was estimated 61.2, 145.2 and 143.8  $\text{m}^2/\text{g}$ , respectively. The corresponding value for pure  $\gamma$ -alumina prepared under the same condition without using  $\text{NaNO}_2$ ,  $\text{HNO}_3$  and  $\text{H}_2\text{SO}_4$  was 150  $\text{m}^2/\text{g}$ . The little change of the specific surface area is observed between the pure  $\gamma$ -alumina and those of modified with  $\text{HNO}_3$ ,  $\text{H}_2\text{SO}_4$ . The specific surface area is drastically reduced for the catalyst treated with  $\text{NaNO}_2$ . The reduced specific surface area of  $\text{NaNO}_2$  doped sample is related to either formation of  $\text{Na}_2\text{O}$  or some Na incorporated in  $\text{Al}_2\text{O}_3$  structure ( $\text{pH}$  near PZC).

**Table 1.** pH measurements of the prepared sol using  $\text{HNO}_3$ ,  $\text{H}_2\text{SO}_4$  and  $\text{NaNO}_2$  before and after reflux.

Mol ratio	0.1 $\text{HNO}_3$	0.5 $\text{HNO}_3$	1 $\text{HNO}_3$	0.5 $\text{H}_2\text{SO}_4$	0.5 $\text{NaNO}_2$
pH of sol before reflux	3.80	1.22	0.63	1.25	8.40
pH of sol after reflux	3.84	3.06	3.14	3.34	8.60

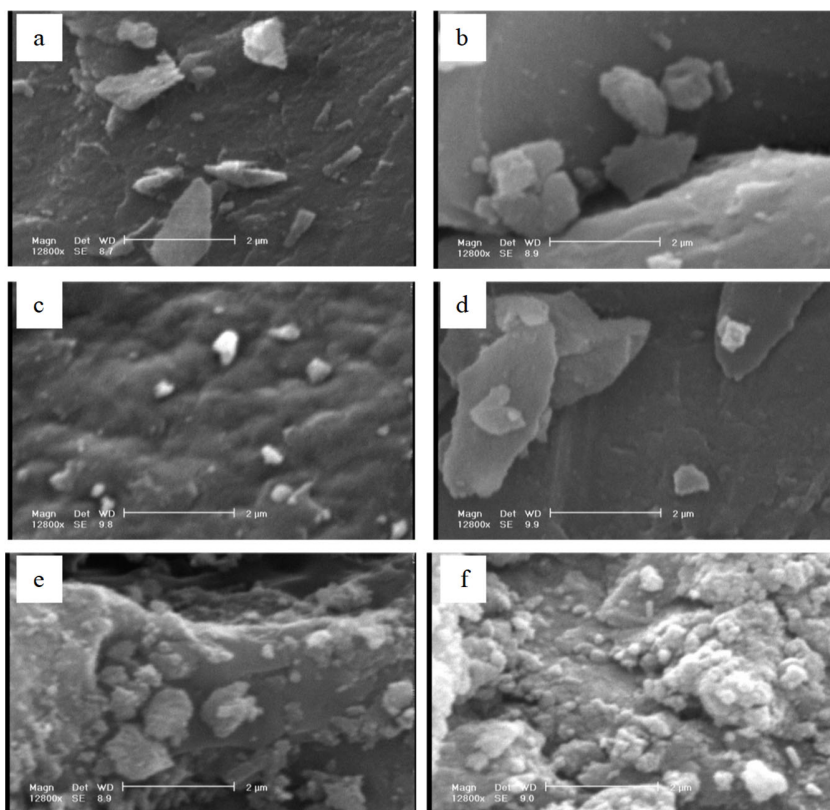


**Fig. 6.** SEM images of the boehmite prepared in 0.5 mol  $\text{H}_2\text{SO}_4$  (top), in 0.5 mol  $\text{HNO}_3$  (middle) and in 0.5 mol  $\text{NaNO}_2$  (bottom) calcined at 350 (left) and 600 °C (right).

The FT-IR spectrum of the dried powder at 120 °C shows absorption at 580  $\text{cm}^{-1}$  (strong), 800  $\text{cm}^{-1}$  (strong), 1640  $\text{cm}^{-1}$  (weak) and a broad band at 2500-3800  $\text{cm}^{-1}$  (strong) that are due to free surface hydroxy groups ( $n\text{OH}$ ) and adsorbed water on the boehmite (Fig. 7a). The latter absorption (broad band) is shifted to 3400  $\text{cm}^{-1}$  (medium) at 350 °C. The intensity is reduced for other signals and resembles  $\gamma$ -alumina. The peaks at 1071  $\text{cm}^{-1}$  and a shoulder at 1153  $\text{cm}^{-1}$  are attributed to the Al-O-H asymmetric and symmetric bending modes [37,38]. The peaks appeared between 625 and 734  $\text{cm}^{-1}$  are assigned to  $\nu\text{-AlO}_4$  and  $\nu\text{-AlO}_6$  corresponding to the tetrahedral and octahedral aluminum atoms.

The FT-IR spectrum of the powder modified with 0.5 mol  $\text{HNO}_3$  solution and heated at 120 °C show strong band at 1350-1380  $\text{cm}^{-1}$  corresponding to  $\text{NO}_3^-$  ion which was lost at 350, and 600 °C (Fig. 7b). The sample calcined at 350 °C under this condition is different that of prepared in water. In this case, polymerization to  $\gamma$ -alumina is incomplete but completed at 600 °C.

The FT-IR of the boehmite prepared in 0.5 mol  $\text{H}_2\text{SO}_4$  solution and heated at 120 °C show a band at 1132  $\text{cm}^{-1}$  corresponding to  $\text{HSO}_4^-$  (Fig. 7c). Strong peaks at 1130 and 1192  $\text{cm}^{-1}$  corresponding to  $3\text{Al}_2\text{O}_3 \cdot 4\text{SO}_4 \cdot x\text{H}_2\text{O}$  of the sample calcined at 350 °C.

This band was disappeared at 600 °C indicating the formation of pure  $\gamma$ -alumina.

The FT-IR of the boehmite prepared in 0.5 mol  $\text{NaNO}_2$  solution and treated at 120 °C show strong band at 1270  $\text{cm}^{-1}$  corresponding to  $\text{NO}_2^-$  (Fig. 7d). Strong peaks at 1384  $\text{cm}^{-1}$  corresponding to  $\text{NaNO}_3$  of the sample calcined at 350 °C.

Recently, it was reported that pure  $\gamma$ -alumina (not modified) converts 44% of 2-octanol into *cis*-2-octene (46%), 1-octene (27%), *trans*-2-octene (23%) and 3-octene (4%) [39]. Conversions of 0.2, 37.3 and 78% 2-octanol were obtained for  $\gamma$ -alumina catalysts modified with  $\text{NaNO}_2$ ,  $\text{HNO}_3$  and  $\text{H}_2\text{SO}_4$ , respectively (Tables 2-4). Drastic decrease in activity and higher selectivity was observed for conversion of 2-octanol over modified alumina by  $\text{NaNO}_2$ . High conversion of 2-octanol in the presence of  $\text{H}_2\text{SO}_4$  is due to increase in acidity of the catalyst. *Cis*-2-octene is the major products of 2-octanol dehydration over catalysts modified by  $\text{NaNO}_2$ ,  $\text{HNO}_3$  and  $\text{H}_2\text{SO}_4$  (Fig. 8, Tables 2-4). The average product selectivity (with low reactivity) for the reaction of 2-octanol over  $\gamma$ -alumina catalysts treated by  $\text{NaNO}_2$  was measured 47.1, 38, 14.9 and 0% for *cis*-2-octene, 1-octene, *trans*-2-octene and 3-octene, respectively.

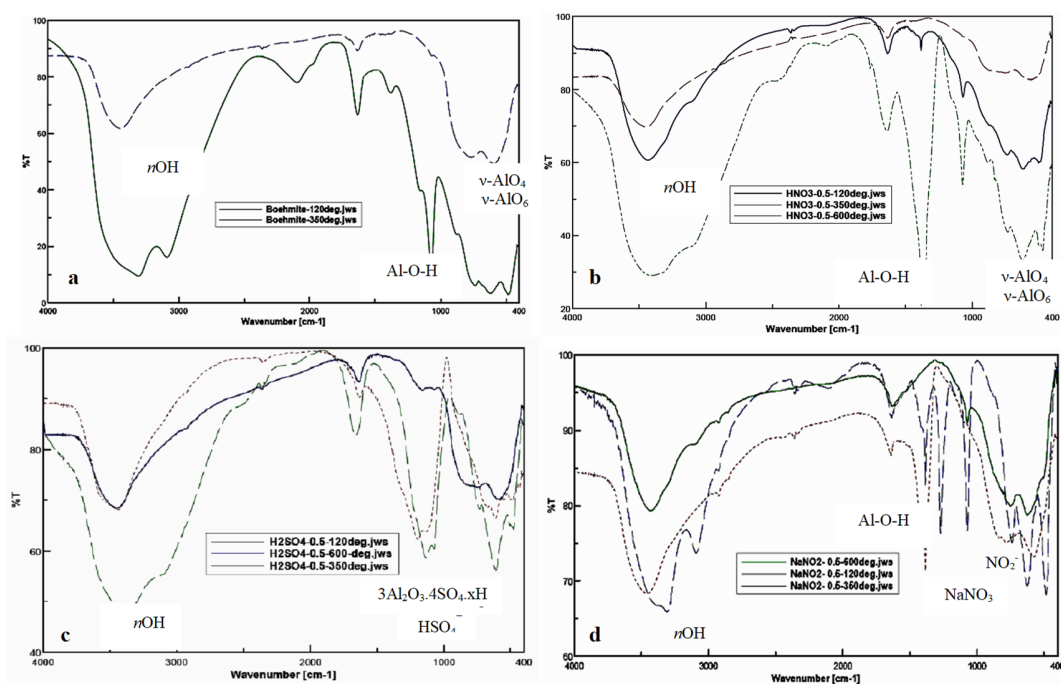


**Fig. 7.** (a) FT-IR of the boehmite prepared in water and treated at 120 and 350 °C. (b) FT-IR of the boehmite prepared in HNO<sub>3</sub> solution and treated at 120, 350, and 600 °C. (c) FT-IR of the boehmite prepared in H<sub>2</sub>SO<sub>4</sub> solution and treated at 120, 350, and 600 °C. (d) FT-IR of the boehmite prepared in NaNO<sub>2</sub> solution and treated at 120, 350, and 600 °C.

**Table 2.** Products selectivity (%) for reaction of 2-octanol over  $\gamma$ -Al<sub>2</sub>O<sub>3</sub> catalyst modified by H<sub>2</sub>SO<sub>4</sub>.

Time (min)	%2-octanol conversion	Selectivity (%)					
		1-octene	<i>trans</i> -2-octene	<i>cis</i> -2-octene	3-octenes	2-octene/1-octene ratio	<i>cis/trans</i> ratio
15	79.9	17.0	25.8	30.5	26.7	3.3	1.2
30	84.0	17.6	25.6	30.5	25.4	3.2	1.2
45	82.6	18.4	25.2	32.8	23.6	3.2	1.3
60	73.0	18.4	25.1	33.5	23.0	3.2	1.3
75	70.0	18.2	25.3	33.8	22.7	3.2	1.3

**Table 3.** Products selectivity (%) for reaction of 2-octanol over  $\gamma$ -Al<sub>2</sub>O<sub>3</sub> catalyst modified by HNO<sub>3</sub>.

Time (min)	%2-octanol conversion	Selectivity (%)					
		1-octene	<i>trans</i> -2-octene	<i>cis</i> -2-octene	3-octenes	2-octene/1-octene ratio	<i>cis/trans</i> ratio
15	40.2	29.0	17.0	45.6	8.1	2.2	2.7
30	40.3	29.6	16.9	46.2	7.4	2.1	2.7
45	38.6	29.3	16.8	46.8	7.2	2.2	2.8
60	32.0	30.0	16.3	47.0	6.7	2.1	2.9
75	39.2	30.4	16.3	46.7	6.6	2.1	2.9
90	33.0	30.5	16.1	47.0	6.4	2.1	2.9

**Table 4.** Products selectivity (%) for reaction of 2-octanol over  $\gamma$ -Al<sub>2</sub>O<sub>3</sub> catalyst modified by NaNO<sub>2</sub>.

Time (min)	Selectivity (%) <sup>a</sup>				
	1-octene	<i>trans</i> -2-octene	<i>cis</i> -2-octene	2-octene/1-octene ratio	<i>cis/trans</i> ratio
15	38.1	15.4	46.5	1.6	3.0
30	38.1	15.0	46.9	1.6	3.1
45	38.0	14.8	47.2	1.6	3.2
60	38.2	14.6	47.2	1.6	3.2
75	38.1	14.8	47.2	1.6	3.2
90	37.8	14.8	47.4	1.6	3.2

\* Overall conversion was less than 10%.

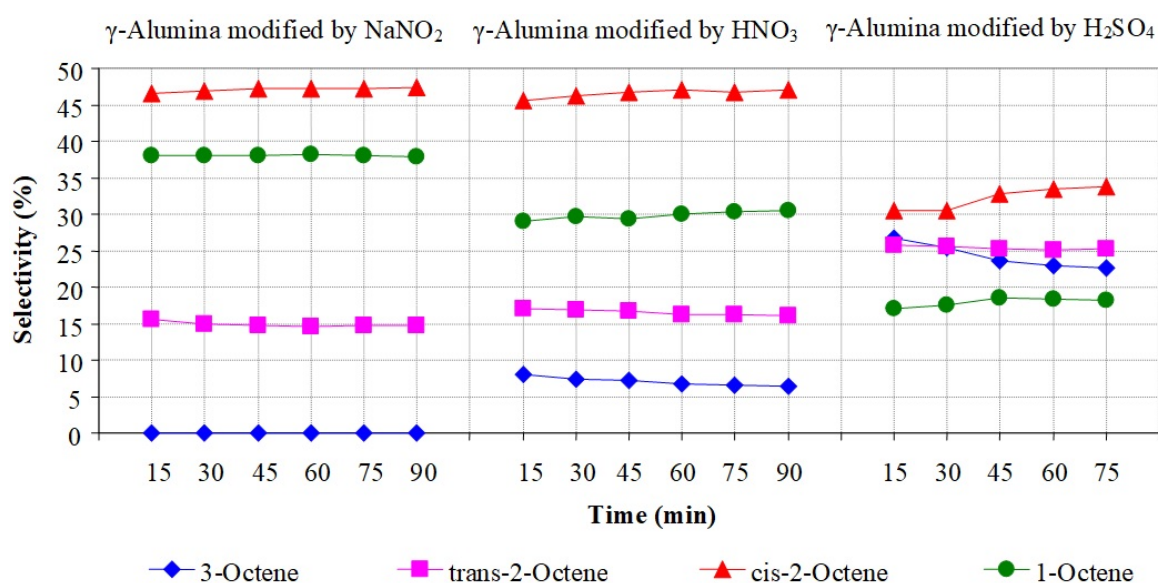


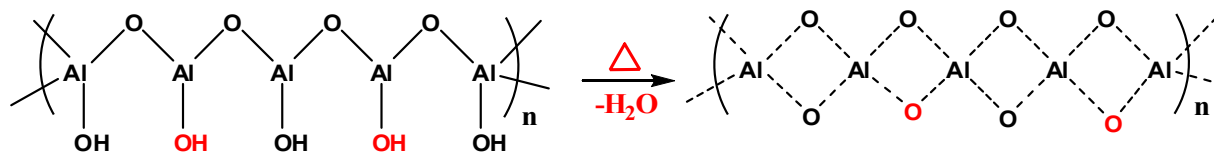
**Fig. 8.** Products selectivity % for dehydration of 2-octanol over modified  $\gamma$ -alumina by NaNO<sub>2</sub>, HNO<sub>3</sub> and H<sub>2</sub>SO<sub>4</sub> (calcined at 600 °C)

For  $\gamma$ -alumina catalyst modified with HNO<sub>3</sub>, the average product selectivity was measured 46.6, 29.8, 16.6 and 7% for *cis*-2-octene, 1-octene, *trans*-2-octene and 3-octene, respectively. The product selectivity over  $\gamma$ -alumina modified with H<sub>2</sub>SO<sub>4</sub> was measured 32.3, 18, 25.4 and 24.3% for *cis*-2-octene, 1-octene, *trans*-2-octene and 3-octene, respectively. The latter sample shows excessive isomerization of 1-octenes and *cis*-2-octenes to 3-octenes and *trans*-2-octene.

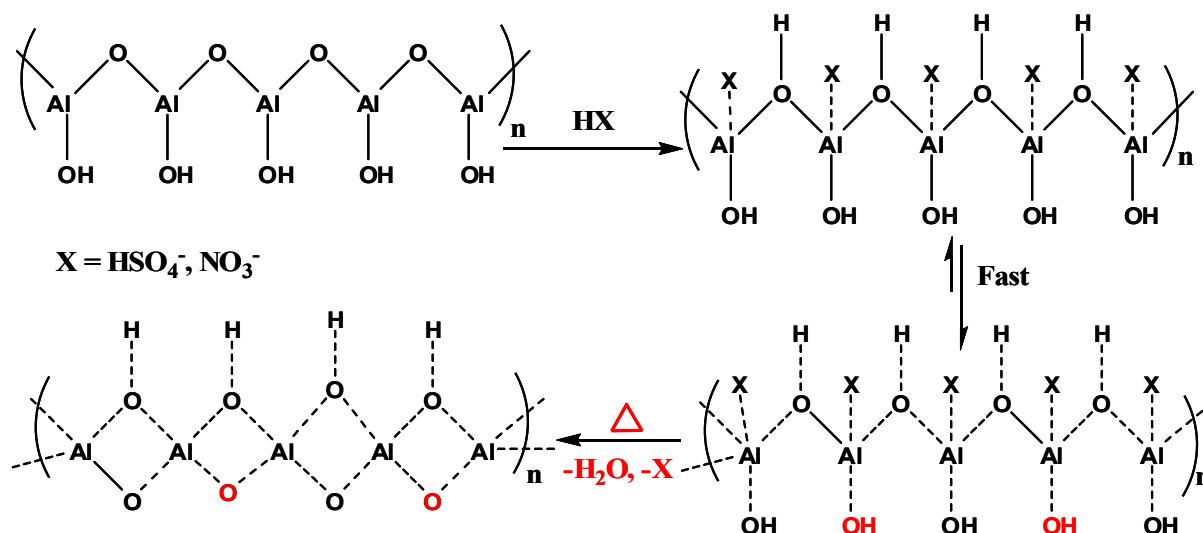
Low conversion and good selectivity for *cis*-2-octene/1-octene ratio and no isomerization was contributed to the modified catalyst with NaNO<sub>2</sub>. The modification with Na enhanced the strength of basic sites (O<sup>2-</sup>) and weakens that of acid sites (Al<sup>3+</sup>) [40]. Schematic representation of the effect of NaNO<sub>2</sub>, HNO<sub>3</sub> and H<sub>2</sub>SO<sub>4</sub> on  $\gamma$ -alumina formation is depicted on Schemes 1-3. Acid treated  $\gamma$ -alumina neutralizes the basic sites (O<sup>2-</sup>) which increases acidity.

#### 4. Conclusions

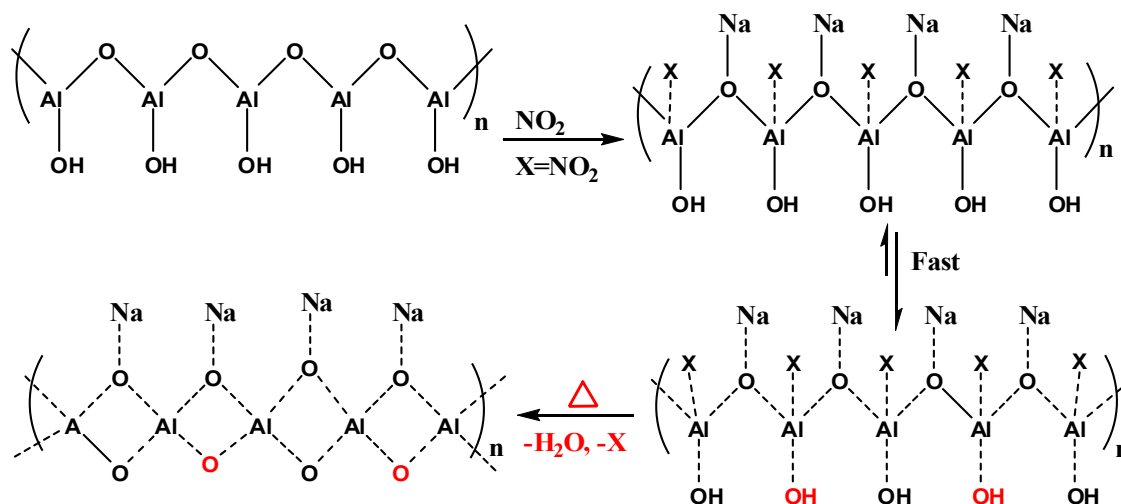
$\gamma$ -Alumina was prepared via a new approach using hydrolysis of aluminum iso-propoxide in the presence of HNO<sub>3</sub>, H<sub>2</sub>SO<sub>4</sub> and NaNO<sub>2</sub>. The pH of solutions was measured after mixing. The influence of NaNO<sub>2</sub>, HNO<sub>3</sub> and H<sub>2</sub>SO<sub>4</sub> on the structure and morphology of  $\gamma$ -alumina was investigated by XRD, BET, SEM and FT-IR spectroscopy. The microstructure of the gel is affected depending on the amount of acid added during the hydrolysis of aluminum iso-propoxide. The peak broadening and reduced specific surface area of the  $\gamma$ -alumina modified with NaNO<sub>2</sub> (calcined at 600 °C) was related to smaller particle size. The XRD pattern of alumina modified with 0.5 mol ratio of H<sub>2</sub>SO<sub>4</sub> (calcined at 350 °C) was drastically broadened in compare to other samples. The influence of NaNO<sub>2</sub>, HNO<sub>3</sub> and H<sub>2</sub>SO<sub>4</sub> on reactivity and selectivity of catalysts were examined using dehydration reaction of 2-octanol; and the results



Scheme 1. Schematic representation of  $\gamma$ -alumina formation.



Scheme 2. Schematic representation of  $\gamma$ -alumina formation in  $\text{HNO}_3$  and  $\text{H}_2\text{SO}_4$ .



Scheme 3. Schematic representation of  $\gamma$ -alumina formation in the presence of  $\text{NaNO}_2$ .

were compared with the conversion of 2-octanol over pure  $\gamma$ -alumina (not modified) catalyst. The dominant product was *cis*-2-octene for all catalysts. Low conversion and higher selectivity were obtained for dehydration of 2-octanol over  $\gamma$ -alumina modified with  $\text{NaNO}_2$ . The catalyst modified with  $\text{H}_2\text{SO}_4$  resulted high

conversion, low selectivity and excessive isomerization of 1-octenes and 2-octenes to 3-octenes. High conversion of 2-octanol in the presence of  $\text{H}_2\text{SO}_4$  is due to increase in acidity of the catalyst. There was a good correlation between reactivity, product selectivity and the amount (and type) of the modification.

## Acknowledgments

We would like to thank the Isfahan University of Technology and Damghan University research council for financial support.

## References

- [1] E.J. Blanc, H. Pines, *J. Org. Chem.* 33 (1968) 2035-2043.
- [2] C.L. Kibby, S.S. Lande, W.K. Hall, *J. Am. Chem. Soc.* 94 (1972) 214-220.
- [3] H. Knozinger, H. Buhl, K. Kochloefl, *J. Catal.* 24 (1972) 57-68.
- [4] H.A. Dabbagh, C.G. Hughes, B.H. Davis, *J. Catal.* 133 (1992) 445-460.
- [5] H.A. Dabbagh, B.H. Davis, *J. Org. Chem.* 55 (1990) 2011-2016.
- [6] B. Shi, H.A. Dabbagh, B.H. Davis, *J. Mol. Catal. A: Chem.* 141 (1999) 257-262.
- [7] H.A. Dabbagh, J. Mohammad Salehi, *J. Org. Chem.* 63 (1998) 7619-7627.
- [8] V. Macho, M. Kralik, E. Jurecekova, J. Hudec, L. Jurecek, *Appl. Catal. A* 214 (2001) 251-257.
- [9] H.A. Dabbagh, M.S. Yalfani, B.H. Davis, *J. Mol. Catal. A: Chem.* 238 (2005) 72-77.
- [10] H.A. Dabbagh, K. Taban, M. Zamani, *J. Mol. Catal. A: Chem.* 326 (2010) 55-68.
- [11] H.A. Dabbagh, M. Zamani, B.H. Davis, *J. Mol. Catal. A: Chem.* 333 (2010) 54-68.
- [12] S. Roy, G. Mpourmpakis, D.Y. Hong, D.G. Vlachos, A. Bhan, R.J. Gorte, *ACS Catal.* (2012) 1846-1853.
- [13] A. Corma, *Chem. Rev.* 95 (1995) 559-614.
- [14] J.B. Peri, *J. Phys. Chem.* 69 (1965) 220-230.
- [15] K. Sohlberg, S.J. Pennycook, S.T. Pantelides, *J. Am. Chem. Soc.* 121 (1999) 7493-7499.
- [16] C. Wolverton, K.C. Hass, *Phys. Rev. B* 63 (2000) 024102.
- [17] X. Krokidis, P. Rayboud, A.E. Gobichon, B. Rebours, P. Euzen, H. Toulhoat, *J. Phys. Chem. B* 105 (2001) 5121-5130.
- [18] M. Digne, P. Sautet, P. Raybaud, P. Euzen, H. Toulhoat, *J. Catal.* 226 (2004) 54-68.
- [19] G. Paglia, C.E. Buckley, A.L. Rohl, B.A. Hunter, R.D. Hart, J.V. Hanna, L.T. Byrne, *Phys. Rev. B* 68 (2003) 144110.
- [20] G. Paglia, A.L. Rohl, C.E. Buckley, G.D. Gale, *Phys. Rev. B* 71 (2005) 224115.
- [21] M. Sun, A.E. Nelson, J. Adjaye, *J. Phys. Chem. B* 110 (2006) 2310-2317.
- [22] A.R. Ferreira, M.J.F. Martins, E. Konstantinova, R.B. Capaz, W.F. Souza, S.S.X. Chiaro, A.A. Leitão, *J. Solid State Chem.* 184 (2011) 1105-1111.
- [23] L. Smrcok, V. Langer, J. Krestan, *Acta Cryst. C* 62 (2006) i83.
- [24] G. Feng, C. Huo, C. Deng, L. Huang, Y. Li, J. Wang, H. Jiao, *J. Mol. Catal. A: Chem.* 304 (2009) 58-64.
- [25] P. Souza Santos, H. Souza Santos, S.P. Toledo, *J. Mater. Res.* 3 (2000) 104-114.
- [26] M.M. Amini, M. Mirzaee, *J. Sol-Gel Sci. Technol.* 36 (2005) 19-23.
- [27] L. Le Bihan, F. Dumeignil, E. Payen, J. Grimblot, *J. Sol-Gel Sci. Technol.* 24 (2002) 113-120.
- [28] Y. Takeda, Y. Hashimoto, H. Nasu, K. Kamiya, *J. Ceram. Soc. Japan* 110 (2002) 1025-1028.
- [29] K. Okada, T. Nagashima, Y. Kameshima, A. Yasumori, T. Takayuki, *J. Colloid Interf. Sci.* 253 (2002) 308-314.
- [30] K.M. Parida, A.C. Pradhan, J. Das, N. Sahu, *Mater. Chem. Phys.* 113 (2009) 244-248.
- [31] Y. Kim, *Sep. Sci. Technol.* 35 (2000) 2327-2341.
- [32] P. Manivasakan, V. Rajendran, P.R. Rauta, B.B. Sahu, B.K. Panda, *Powder Technol.* 211 (2011) 77-84.
- [33] M. Zamani, H.A. Dabbagh, *Iran. J. Catal.* 6 (2016) 345-353.
- [34] P. Alphonse, M. Courty, *J. Colloid Interf. Sci.* 290 (2005) 208-219.
- [35] D. Fauchadour, F. Kolenda, L. Rouleau, L. Barre, L. Normand, *Stud. Surf. Sci. Catal.* 143 (2002) 453-461.
- [36] C.R. Evanko, R.F. Delisio, D.K. Dzombak, J.W. Novak Jr., *Colloids Surf. A Physicochem. Eng. Aspects* 125 (1997) 95-107.
- [37] G. Zu, J. Shen, L. Zou, W. Wang, Y. Lian, Z. Zhang, A. Du, *Chem. Mater.* 25 (2013) 4757-4764.
- [38] G. Zu, J. Shen, X. Wei, X. Ni, Z. Zhang, J. Wang, G. Liu, *J. Non-Cryst. Solids* 357 (2001) 2903-2906.
- [39] H.A. Dabbagh, M. Zamani, *Appl. Catal. A* 404 (2011) 141-148.
- [40] T. Seki, S. Ikeda, M. Onaka, *Microporous Mesoporous Mater.* 96 (2006) 121-126.